



CHORUS

This is the accepted manuscript made available via CHORUS. The article has been published as:

Pulsed Entanglement of Two Optomechanical Oscillators and Furry's Hypothesis

S. Kieseletter, R. Y. Teh, P. D. Drummond, and M. D. Reid

Phys. Rev. Lett. **119**, 023601 — Published 13 July 2017

DOI: [10.1103/PhysRevLett.119.023601](https://doi.org/10.1103/PhysRevLett.119.023601)

Pulsed entanglement of two optomechanical oscillators and Furry’s hypothesis

S. Kiesewetter, R. Y. Teh, P. D. Drummond and M. D. Reid

Center for Quantum and Optical Science, Swinburne University of Technology, Melbourne, Australia

A strategy for generating entanglement between two separated optomechanical oscillators is analyzed, using entangled radiation produced from downconversion and stored in an initiating cavity. We show that the use of pulsed entanglement with optimally shaped temporal modes can efficiently transfer quantum entanglement into a mechanical mode, then remove it after a fixed waiting time for measurement. This protocol could provide new avenues to test for bounds on decoherence in massive systems that are spatially separated, as originally suggested by Furry [1] not long after the discussion by Einstein-Podolsky-Rosen (EPR) and Schrödinger of entanglement.

Macroscopic mechanical oscillators have now been cooled to their quantum ground state [2–5], followed by the observations of macroscopic quantum effects [6–9] including quantum entanglement [10] between a mechanical oscillator and a radiation field. Even more spectacular demonstrations of macroscopic quantum properties will soon become achievable [11–14]. An important goal is to demonstrate long-lived entanglement between two separated mechanical systems. This would enable new tests of quantum mechanics, including the possible decoherence of EPR entanglement with space-like separation.

The intriguing idea of spatially dependent decoherence [1] was proposed by Furry just after the publication of the original EPR paradox [15] and entanglement papers [16]. This hypothesis (called Method A in Furry’s paper) is not predicted by conventional quantum mechanics. It could occur in a modified quantum mechanics, that includes quantum gravity or other types of intrinsic decoherence. This differs from the well-known proposals [17–20] which focus on the collapse of the wavefunction of a macroscopic superposition state. Experiments show that spatially dependent decoherence is not observed for massless photons [21], although calculations suggest a small decay due to space-time curvature [22]. However, there are no measurements yet of such entanglement decay with massive, separated objects having an entangled center-of-mass motion. Experiments would enable bounds to be placed on the parameters leading to a mass-dependent decay of entanglement in Furry decoherence models [23]. Gravity-wave detectors [24] and optomechanical entanglement [10] demonstrate the possibility of investigating questions like this.

In this Letter, we propose and analyze a simple pulsed protocol for creating and measuring such macroscopic entanglement. The basic experimental setup involves an entangled source and spatially separated quantum optomechanical systems. An optical parametric amplifier creates two entangled modes [25–28], ideally with the same frequency and different polarizations. This entanglement is transferred, on demand, to the separated quantum optomechanical systems – thus destroying the initial entanglement in optical modes. The entangled mechanical

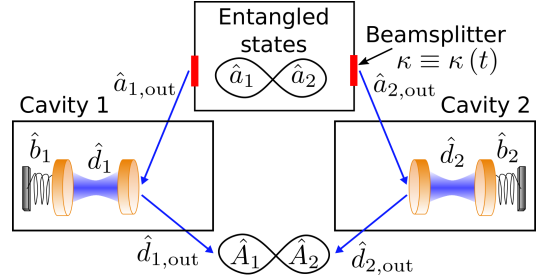


Figure 1. Schematic diagram of entanglement protocol.

modes are stored, subsequently coupled out and measured optically, as shown in Fig (1). Other proposals for entangling quantum optomechanical systems have been suggested [11, 12, 29–33]. However, these do not give a way to control the lifetime of quantum entanglement and spatial separation of massive oscillators, combined with an efficient intracavity state transfer mechanism – as has recently been exploited experimentally to demonstrate a coherent state memory [10, 34]. These requirements appear essential to a test of Furry’s hypothesis.

The entangled source cavity modes a_1 and a_2 are assumed to be initially in a two mode squeezed state, prepared using the standard technique of nondegenerate parametric down-conversion. To give a definite model, this entangled state is initially prepared in a source cavity whose entanglement is characterized by a squeezing parameter r . The source cavity has tunable decay rates $\kappa(t)$, generating shaped, entangled outputs [35, 36]. This approach, using cavity Q-switching [37], is the simplest conceptually; we note that other methods involving time-dependent cavity detunings are also possible [35].

The resulting entangled fields are fed [38–40] into the quantum optomechanical systems labelled Cavity 1 and Cavity 2, respectively, assuming identical optomechanical parameters. For simplicity, we linearize the equations of motion for an adiabatic [29, 30] pulsed optomechanical Hamiltonian describing these devices [31, 41–43], including dissipation and thermal noise for the cavity and mechanical modes, and we verify this approach using exact methods. A time dependent optomechanical interaction $g(t)$ [35] allows the entangled modes to transfer to

and from the mechanical modes \hat{b}_1 and \hat{b}_2 . The internal mechanical entanglement is read out via additional red-detuned transfer pulses that enter the opto-mechanical cavities after a storage time τ_s , as used in coherent state transfer experiments [34]. These are shaped optimally for maximum retrieval efficiency [35, 36], with subsequent measurement of the stored entanglement using homodyne detection.

Time-dependent coupling and decay The optomechanical systems are modeled using the standard single mode theory [44–46], following techniques explained in previous papers [41]. It is convenient to introduce a dimensionless time variable, $\tau = \Gamma_c t$, relative to the optomechanical cavity decay rate Γ_c . To obtain universally valid results covering a range of different cases, all other times, frequencies and couplings are given in dimensionless units with derivatives $\dot{f} \equiv \partial f / \partial \tau$.

The equations of motion for the source cavity mode operators a_1, a_2 , are obtained in the absence of thermal noise, assuming the only losses are due to input/output coupling with a transmissivity $\kappa(\tau)$. Using input-output theory, with inputs $a_{k,\text{in}}$ and outputs $a_{k,\text{out}}$ one obtains [47, 48]:

$$\begin{aligned} \dot{a}_k &= -\kappa(\tau) a_k + \sqrt{2\kappa(\tau)} a_{k,\text{in}} \\ a_{k,\text{out}} &\equiv \sqrt{2\kappa(\tau)} a_k - a_{k,\text{in}}. \end{aligned} \quad (1)$$

We wish to generate a sech shaped output pulse, $a_{\text{out}} \propto \text{sech}(\tau)$. This is achieved using a dimensionless mirror transmissivity defined according to $\kappa(\tau) = [1 + \tanh(\tau)]/2$. We solve for Eq. (1), giving

$$\begin{aligned} a_k &= a_k(-\infty) \sqrt{\left[\frac{1 - \tanh(\tau)}{2} \right]} + a_{\text{vac}} \\ a_{k,\text{out}} &= \frac{a(-\infty)}{\sqrt{2}} \text{sech}(\tau) + a'_{\text{vac}}. \end{aligned} \quad (2)$$

The operators $a_{\text{vac}}, a'_{\text{vac}}$ are the source input and output vacuum noises respectively. The cavities are cascaded, so $d_{k,\text{in}} = a_{k,\text{out}}$, and from the input-output relations, $d_{k,\text{out}} \equiv \sqrt{2}d_k - d_{k,\text{in}}$. The optomechanical systems satisfy the standard quantum Langevin equations [41, 44] with cavity detuning $\delta\omega$, mechanical loss γ_m , and optomechanical coupling χ , in dimensionless units.

The full nonlinear optomechanical Hamiltonian in dimensionless terms is $H_{NL} = g_0 d^\dagger d (b + b^\dagger)$. Assuming an intense red-detuned pump with $\delta\omega = \omega_m$, and a resulting adiabatic coupling of $g = i\chi E / (1 + i\delta\omega)$, the linearized Hamiltonian for cavities 1 and 2 becomes $\hat{H}_{a,k} \approx i(g^* d_k b_k^\dagger - g d_k^\dagger b_k)$. Here, d_k is a small fluctuation around the steady state in a frame rotating with detuning $\delta\omega$. We determine the time dependence of the optomechanical interaction strengths $g(\tau)$ of cavities 1 and 2, from previous work on quantum memories [36].

To understand the mode-matching method, we start by

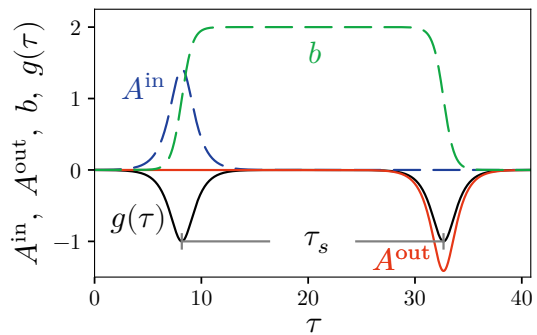


Figure 2. Temporal behavior of the input field a_{in} , the output field A_{out} , the mechanical state b and the coupling strength $g(\tau)$.

analyzing the linearized equations without losses in the mechanical oscillator, and without vacuum noise terms. These will be included in the full numerical analysis, given next. At this stage, we have that:

$$\begin{aligned} \dot{d}_k &= -d_k - ig(\tau) b_k + \sqrt{2}d_{k,\text{in}} \\ \dot{b}_k &= -ig(\tau) d_k. \end{aligned} \quad (3)$$

To find conditions for perfect input coupling, we require that $d_{\text{out}} = 0$ in the absence of vacuum noise. Hence $d_{k,\text{in}} = \sqrt{2}d_k$, leading to $\dot{d}_k = d_k - ig(\tau) b_k$. If we further assume $b_{-\infty} = 0$, again neglecting vacuum noise, then it follows that $-ig(\tau) = \dot{b}_k/d_k$, giving

$$\left(\dot{d}_k + igb_k \right) / d_k = \dot{d}_k/d_k - \left(\dot{b}^2 \right) / (2d_k^2) = 1. \quad (4)$$

Now we note that $d_k = a(-\infty) \text{sech}(\tau)/2$, and solving Eq. (4) gives us $b_k = ia(-\infty) [1 + \tanh(\tau)]/2$. From $-ig(\tau) = \dot{b}_k/d_k$, we obtain the input modulation requirement of $g(\tau) = -\text{sech}(\tau - \tau_1)$, where τ_1 is the peak transmission of the input. The output modulation is identical apart from a shifted time-origin, from the symmetry of the input/output relations under interchange of the input and output terms. The pulse protocol is shown in Fig (2).

Output modes \hat{A}_1, \hat{A}_2 In order to ensure the entanglement is stored in the mechanical, not the optical mode, we suppose there is a separation of time-scales with a relatively long storage time of $\tau_s \gg 1$, so that any optical excitation and entanglement has decayed. We also assume that the mechanical dissipation rate γ_m is small during the storage time, i.e $\gamma_m \tau_s \ll 1$. Detecting the stored entanglement requires an output measurement on temporal modes $\hat{A}_k = \int_{-\infty}^{\infty} u_k(\tau') \hat{d}_{\text{out}}(\tau') d\tau'$ such that $[\hat{A}_k, \hat{A}_k^\dagger] = 1$ [31]. We can then observe entanglement between \hat{A}_1 and \hat{A}_2 on a scale comparable with the initial entanglement between \hat{a}_1 and \hat{a}_2 . Choosing the output pulse to be an identical shape to the input, so that $\hat{a}_{k,\text{out}} \propto \text{sech}(\tau)$, we have $u_k(\tau) = u(\tau) = N \cdot \text{sech}(\tau)$.

This leads to a normalization of

$$N = 1/\sqrt{\int_{-\infty}^{\infty} \text{sech}(\tau)^2 d\tau} = \sqrt{\frac{1}{2}}, \quad (5)$$

The normalization constant for a restricted time-domain can also be found, which leads to minor corrections.

Wigner representation and stochastic equations
There is thermal noise in the mechanical mode due to the interaction with its reservoir. In order to simulate these effects, and to include vacuum noise terms rigorously, it is useful to introduce a quantum phase-space representation of the system density matrix [49]. Initially we choose the Wigner distribution, which for the initial entangled state is given by [50]

$$W(\alpha_+, \alpha_-, \tau_0) = \frac{4}{\pi^2} \exp \left[-2 \left(\frac{|\alpha_+|^2}{e^{2r}} + \frac{|\alpha_-|^2}{e^{-2r}} \right) \right]. \quad (6)$$

Here $\alpha_{\pm} = (\alpha_1 \pm \alpha_2^*)/\sqrt{2}$ and r is the squeezing parameter that characterizes the degree of entanglement. Since this has a Gaussian probability distribution, one can readily simulate the experimental protocol by generating Gaussian noise vectors ξ_x^{\pm}, ξ_y^{\pm} with unit variance, defining $\alpha_{\pm} = [\xi_x^{\pm} + i\xi_y^{\pm}] e^{\pm r}/2$ and then obtaining mode amplitudes $\alpha_1 = (\alpha_+ + \alpha_-)/\sqrt{2}$ and $\alpha_2 = (\alpha_+^* - \alpha_-^*)/\sqrt{2}$. It is also possible to use a positive-P representation [51], which allows an exact simulation of the full nonlinear Hamiltonian \hat{H}_{NL} , with no approximations apart from sampling [41]. For reasons of space, the full analysis will be given elsewhere, but the results are plotted here.

Quantum dynamical time evolution now follows a stochastic equation. Taking account of the cascaded input-output relations, the coupled equations describing time evolution of the Wigner amplitudes for the entangled source cavities α_k , optical cavities δ_k and mechanical modes β_k are given, for $k = 1, 2$, by

$$\begin{aligned} \dot{\alpha}_k &= -\kappa(\tau) \alpha_k + \sqrt{2\kappa(\tau)} \xi_k \\ \dot{\delta}_k &= -\delta_k - ig(\tau) \beta_k + 2\sqrt{\kappa(\tau)} \alpha_k - \sqrt{2} \xi_k \\ \dot{\beta}_k &= -\gamma_m \beta_k - ig(\tau) \delta_k + \sqrt{2\gamma_m (2\bar{n}_{th,m} + 1)} \xi_{2+k}. \end{aligned} \quad (7)$$

Here $\bar{n}_{th,m} = 1/[\exp(\hbar\Gamma_c\omega_m/k_B T) - 1]$ is the average phonon number in the mechanical bath, and ξ_k are complex Gaussian noises with variances that correspond to the 'half-quanta' occupations of symmetric Wigner vacuum correlations, $\langle \xi_k(\tau) \xi_l^*(\tau') \rangle = \frac{1}{2} \delta_{kl} \delta(\tau - \tau')$. Using the input-output relations again, we obtain the expression $\delta_{k,out} = \sqrt{2} \delta_k - \sqrt{2\kappa(\tau)} \alpha_k + \xi_k$. The output modes used for detecting entanglement are then:

$$\begin{aligned} A_{k,out} &= \int_{\tau_1 + \tau_s/2}^{\tau_{max}} u(\tau - \tau_2) \\ &\times \left(\left[\sqrt{2} \delta_k - \sqrt{2\kappa(\tau)} \alpha_k \right] + \xi_k \right) d\tau. \end{aligned} \quad (8)$$

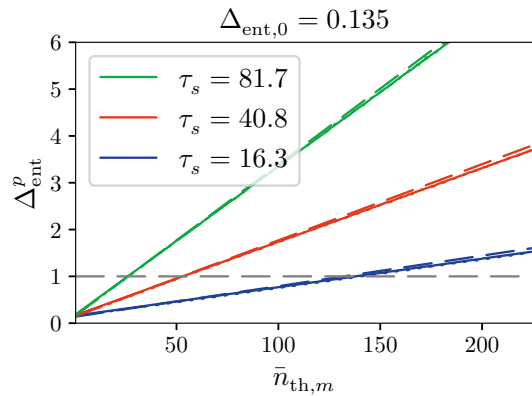


Figure 3. Entanglement as a function of temperature for three different storage times. The initial squeezing parameter is $r = 1$, characterizing the degree of entanglement in the source cavity, while $\Delta_{ent,0} = 0.135$ is the initial value of entanglement. Sloping dashed lines represent the analytic approximation, solid lines the exact positive-P simulation results including the full nonlinearity, and the dotted lines are the truncated Wigner approximate simulations.

Note that the time integration for the output modes only starts after the first transfer pulse has been completed.

Experimental parameters We assume that the optical modes of cavities 1 and 2 are initially in a vacuum state. The source cavity and cavities 1 and 2 are connected by a perfect, lossless waveguide.

Our simulations used experimental parameter values very similar to the optomechanical experiment values reported by Chan et. al. [3]. The mechanical modes have an initial occupation of $n_{th,b}(0) = 0.7$, corresponding to a reservoir temperature of 200 mK. The cavity decay rate is $\Gamma_c/2\pi = 0.26$ GHz. Relative to this time-scale, the mechanical oscillator has dimensionless resonance frequency $\omega_m/2\pi = 14.23$, with a mechanical dissipation rate of $\gamma_m/2\pi = 1.59 \cdot 10^{-5}$ and an optomechanical coupling strength of $\chi_0/2\pi = 3.5 \cdot 10^{-3}$, which justifies the linearization [29, 30] and adiabatic approximations [31].

The time dependent source cavity decay rate that shapes the entangled modes is given by $\kappa(\tau) = \frac{1}{2} [1 + \tanh(\tau - \tau_1)]$, while the effective coupling strength is

$$g(\tau) = \begin{cases} -\sqrt{2}u(\tau - \tau_1), & \forall 0 \leq \tau \leq \tau_1 + \frac{\tau_s}{2} \\ -\sqrt{2}u(\tau - \tau_2), & \forall \tau_1 + \frac{\tau_s}{2} \leq \tau \leq \tau_{max}, \end{cases} \quad (9)$$

where $\tau_1 = 8.17$ and $\tau_2 = \tau_1 + \tau_s$ are the dimensionless times when the storing and reading pulses peak, and $\tau_{max} = 2\tau_1 + \tau_s$, while τ_s is the dimensionless time between the peaks of the storage and readout pulses. It is also the storage time of the entangled state in the mechanical mode, as illustrated in Fig. 2.

Entanglement criterion We use the phase- and gain-optimized product signature as an entanglement criterion

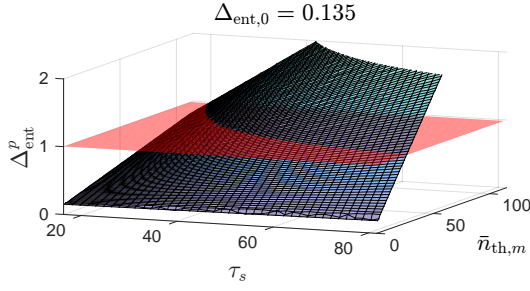


Figure 4. Entanglement as a function of temperature and storage time. Results are obtained using the truncated Wigner method, other parameters as in Fig (3).

[52], defined as:

$$\Delta_{ent}^p = \frac{4\Delta (X_1 - GX_2^\theta) \Delta (P_1 + GP_2^\theta)}{(1 + G^2)} < 1, \quad (10)$$

where $X_k^\theta = \frac{1}{2} [e^{-i\theta} A_{k,\text{out}} + e^{i\theta} A_{k,\text{out}}^\dagger]$, $P_k^\theta = X_k^{\theta+\pi/2}$ and G is an adjustable real constant. In particular, $X_k = X_k^0$, $P_k = P_k^0$ are the usual phase and amplitude quadratures. We minimize Δ_{ent}^p with respect to the gain G and phase θ simultaneously. When inequality (10) holds, the optimized value of Δ_{ent}^p characterizes the degree of quantum entanglement between the modes [53].

We compute Δ_{ent}^p in Eq. (10) as a function of thermal reservoir occupation number for a set of different storage times and a fixed squeezing parameter. To give an approximate analytic prediction, we consider only the degradation of the entanglement during its storage period in the mechanical oscillators. Using results described in [54], we predict an entanglement value of

$$\Delta_{ent}^p = e^{-2\gamma_m \tau_s} e^{-2r} + (1 - e^{-2\gamma_m \tau_s}) (1 + 2\bar{n}_{\text{th},m}). \quad (11)$$

Fig. (3) shows the predicted entanglement results for squeezing parameter $r = 1$ and three different storage times $\tau_s = 16.3, 40.8, 81.7$, corresponding to 10 ns, 25 ns and 50 ns, respectively. The dotted and solid lines indicate simulation results and dashed lines theoretical predictions.

The truncated Wigner simulation results in the dotted lines were obtained by solving Eqs. (7) with a stochastic 4-th order Runge-Kutta algorithm, 3000 time-steps and $\approx 2 \cdot 10^8$ samples, using open-source software [55]. They are in good agreement with our analytic predictions. Results for an exact positive-P simulation of the full nonlinear optomechanical model, with neither adiabatic nor linearization approximations, are also given (solid line of Fig 3). These used 10^4 time steps, and give essentially the same results, showing that quantum predictions for this system can be calculated quantitatively. A larger initial entanglement in the source cavity and a shorter storage

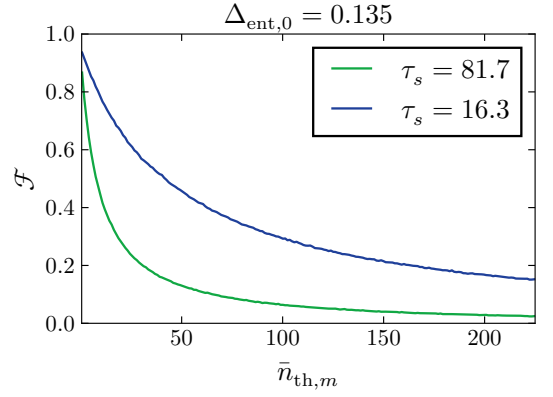


Figure 5. Fidelity \mathcal{F} as a function of the thermal bath occupation number and storage time. Other parameters as in Fig 4.

time gives even better output temporal mode entanglement. Fig. (4) gives a three-dimensional representation of the truncated Wigner results against storage time and temperature, showing how higher mechanical temperatures more rapidly degrade entanglement.

Quantum fidelity We consider the quantum fidelity measure $\mathcal{F} = \langle \psi | \rho | \psi \rangle$, where $|\psi\rangle$ is the two mode squeezed state and ρ is the density operator describing the temporal output modes. The fidelity quantifies the efficiency of our entanglement protocol as the entanglement in output temporal modes rely on successful entangled state transfer from the source cavity. In the Wigner representation [56, 57],

$$\mathcal{F} = \pi^2 \int W_\psi(\alpha_1, \alpha_2) W_\rho(\alpha_1, \alpha_2) d^2\alpha_1 d^2\alpha_2. \quad (12)$$

From the quantum simulations, we obtain sampled temporal output modes from the Wigner function W_ρ . The quantum fidelity \mathcal{F} is then computed using

$$\mathcal{F} = \frac{\pi^2}{N_{\text{sample}}} \sum_i W_\psi(A_{1,\text{out}}^i, A_{2,\text{out}}^i), \quad (13)$$

where $A_{k,\text{out}}^i$ is the i -th sample of temporal output mode $A_{k,\text{out}}$ and N_{sample} is the total number of samples taken.

The quantum fidelity in Eq. (13) is also computed as a function of reservoir temperature and storage time, showing the steep drop in fidelity as storage time is increased. Comparing plots in Fig. (4) and Fig. (5) shows that a fidelity \mathcal{F} of at least about 0.3 is needed for entangled output modes.

EPR-steering In addition to entanglement, we also analyze the stronger, asymmetric nonlocality signature known as the EPR-steering that links directly to the EPR paradox [15, 25, 58]. We use the CV signature for steering of system 1 by system 2 [25]

$$EPR_{1|2} = 4\Delta (X_1 - GX_2^\theta) \Delta (P_1 + GP_2^\theta) < 1, \quad (14)$$

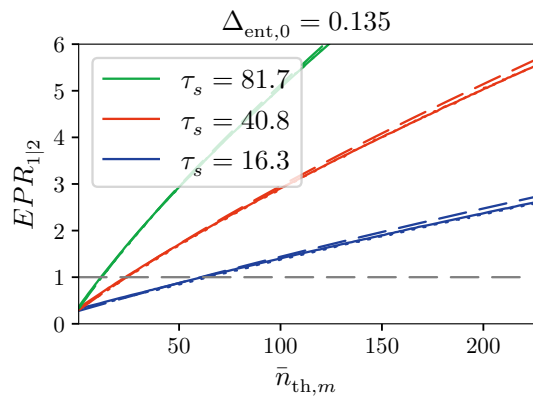


Figure 6. EPR-steering as a function of the thermal bath occupation number for three different storage times. Other parameters as in Fig 3.

with X , P as previously and an optimized gain G . Fig. 6 shows the predicted results for EPR-steering. The solid lines indicate simulation results and the dashed lines give analytic predictions. The analytic predictions were obtained analogously to the entanglement predictions. Using the results described in [54], we obtain

$$EPR_{1|2} = \frac{2ab(1-b)c + b^2 + c^2(1-b)^2}{ab + (1-b)c}, \quad (15)$$

where $a \equiv \cosh(2r)$, $b \equiv e^{-2\gamma_m\tau_s}$, $c \equiv (1 + 2\bar{n}_{th,m})$. Because of the symmetric setup, $EPR_{1|2}$ and $EPR_{2|1}$ are equal in magnitude. Both approximate truncated Wigner and exact positive-P results were obtained here, giving excellent agreement with the analytic theory for these parameter values.

Conclusions In summary, our results show that a synchronous pulsed experiment can, in principle, transfer, store and read out macroscopic entanglement of two mechanical oscillators with nearly 100% efficiency under ideal conditions. Due to finite temperature effects and damping, this effect is degraded in a predictable way. We calculate the quantitative effects of known decoherence on this proposed experiment. The experimental objectives would be to demonstrate entanglement transfer, and hence place a bound on any decoherence rate caused by the oscillator separation, to test the validity of models that implement Furry's hypothesis.

This research was supported in part by the National Science Foundation under Grant NSF PHY-1125915, and by the Australian Research Council under Grant DP140104584.

[1] W. H. Furry, Phys. Rev. **49**, 393 (1936).
 [2] A. D. O'Connell et al., Nature **464**, 697 (2010).
 [3] J. Chan et al., Nature **478**, 89 (2011).

[4] S. Groblacher et al., Nature Physics **5**, 485 (2009).
 [5] J. D. Teufel et al., Nature **475**, 359 (2011); **471**, 204 (2011).
 [6] A. Safavi-Naeini et al, Phys. Rev. Lett. **108**, 033602 (2012).
 [7] N. Brahms, T. Botter, S. Schreppler, D. W. C. Brooks, D. M. Stamper-Kurn, Phys. Rev. Lett. **108**, 133601 (2012).
 [8] T. J. Kippenberg and K. J. Vahala, Science **321**, 1172 (2008).
 [9] M. Aspelmeyer et al., J. Opt. Soc. Am. B **27**, A189 (2010).
 [10] T. A. Palomaki et al., Science **342**, 710 (2013).
 [11] W. Marshall, C. Simon, R. Penrose and D. Bouwmeester, Phys. Rev. Lett. **91**, 130401 (2003).
 [12] S. Pirandola, D. Vitali, P. Tombesi, and S. Lloyd, Phys. Rev. Lett. **97**, 150403 (2006).
 [13] A. Mari, G. De Palma, and V. Giovannetti, Sci. Rep. **6**, 22777 (2016).
 [14] C. Wan et al., Phys. Rev. Lett. **117**, 143003 (2016).
 [15] A. Einstein, B. Podolsky, and N. Rosen, Phys. Rev. **47**, 777 (1935).
 [16] E. Schrödinger, Naturwissenschaften **23**, 844 (1935).
 [17] P. Pearle, Phys. Rev. D **13**, 857 (1976); **29**, 235 (1984); **33**, 2240 (1986); Phys. Rev. A **39**, 2277 (1989).
 [18] G. C. Ghirardi, A. Rimini, and T. Weber, Phys. Rev. D **34**, 470 (1986); G. C. Ghirardi, R. Grassi, A. Rimini, Phys. Rev. A **42**, 1057 (1990).
 [19] R. Penrose, Gen. Rel. and Grav. **28**, 581 (1996). R. Penrose, Philos. Trans. R. Soc. London, Ser. A **356**, 1927 (1998).
 [20] L. Diosi, Phys. Lett. A **120**, 377 (1987); L. Diosi, Phys. Rev. A **40**, 1165 (1989); L. Diosi, J. Phys. A: Math. Theor. **40**, 2989 (2007).
 [21] B. Hensen et al., Nature **526**, 682 (2015).
 [22] T.C. Ralph, G.J. Milburn and T. Downes, arXiv:quant-ph/0609139v2 (2007).
 [23] P. D. Drummond and M. D. Reid, Presented at 605 WE-Heraeus-Seminar (Physikzentrum Bad Honnef, Germany, 17–22 January, 2016)
 [24] B. P. Abbott et al. , Phys. Rev. Lett. **116**, 061102 (2016).
 [25] M. D. Reid, Phys. Rev. A **40**, 913 (1989).
 [26] M. D. Reid, P. D. Drummond, Phys. Rev. A **40**, 4493 (1989); P. D. Drummond, M. D. Reid, Phys. Rev. A **41**, 3930 (1990).
 [27] Z. Y. Ou, S. F. Pereira, H. J. Kimble, K. C. Peng, Phys. Rev. Lett. **68**, 3663 (1992); W. P. Bowen, R. Schnabel, P. K. Lam, T. C. Ralph, Phys Rev. Lett. **90**, 043601 (2003); K. Wagner *et al.*, Science **321**, 541 (2008).
 [28] M. D. Reid *et al.*, Rev. Mod. Phys. **81**, 1727 (2009).
 [29] V. Giovannetti, S. Mancini and P. Tombesi, Europhys. Lett. **54**, 559 (2001).
 [30] S. Mancini, V. Giovannetti, D. Vitali and P. Tombesi, Phys. Rev. Lett. **88**, 120401 (2002).
 [31] S. G. Hofer, W. Wiczorek, M. Aspelmeyer, K. Hammerer, Phys. Rev. A **84**, 052327 (2011).
 [32] Q. Y. He and M. D. Reid, Phys. Rev. A **88**, 052121 (2013).
 [33] A. Asadian, C. Brukner, and P. Rabl, Phys. Rev. Lett. **112**, 190402 (2014).
 [34] T. Palomaki, J. Harlow, J. Teufel, R. Simmonds, and K. Lehnert, Nature **495**, 210 (2013).
 [35] Q. Y. He, M. D. Reid, E. Giacobino, J. Cviklinski and P. D. Drummond, Phys. Rev. A **79**, 022310 (2009).

- [36] Q. Y. He, M. D. Reid, and P. D. Drummond, *Opt. Express* **17**, 9662 (2009).
- [37] John D. Simon, *Review of Scientific Instruments* **60**, 3597 (1989).
- [38] M. I. Kolobov and I. V. Sokolov, *Opt. Spektrosk.* **62**, 112 (1987).
- [39] H. J. Carmichael, *Phys. Rev. Lett.* **70**, 2273 (1993).
- [40] C. W. Gardiner, *Phys. Rev. Lett.* **70**, 2269 (1993).
- [41] S. Kiesewetter, Q.Y. He, P. D. Drummond and M.D. Reid, *Phys. Rev. A* **90**, 043805 (2014).
- [42] M. R. Vanner et al., *Proc. Nat. Ac. Sc.* **108**, 16182 (2011).
- [43] I. Pikovski et al., *Nat. Phys.* **8**, 393 (2012).
- [44] A. F. Pace, M. J. Collett, D. F. Walls, *Phys. Rev. A* **47**, 3173 (1993). The standard model described here uses approximations such as the Markovian approximation.
- [45] V. B. Braginsky and A. Manukin, *Sov. Phys. JETP* **25**, 653 (1967).
- [46] A. Dorsel, J. D. McCullen, P. Meystre, E. Vignes and H. Walther, *Phys. Rev. Lett.* **51**, 1550 (1983).
- [47] B. Yurke, *Phys. Rev. A* **32**, 300 (1985).
- [48] C. W. Gardiner and M. J. Collett, *Phys. Rev. A* **31**, 3761 (1985); M. J. Collett and D. F. Walls, *ibid.* **32**, 2887 (1985).
- [49] E. P. Wigner, *Phys. Rev.* **40** 749 (1932); R. Graham, in *Springer Tracts in Modern Physics: Quantum Statistics in Optics and Solid-State Physics*, edited by G. Hohler, (Springer, New York, 1973).
- [50] D. Walls and G. Milburn, *Quantum Optics* 2nd edition (Springer, 2008).
- [51] P. D. Drummond and C. W. Gardiner, *J. Phys. A: Math. Gen.* **13**, 2353 (1980).
- [52] V. Giovannetti, S. Mancini, D. Vitali and P. Tombesi *Phys. Rev. A* **67**, 022320 (2003).
- [53] Q. Y. He, Q. H. Gong, and M. D. Reid, *Phys. Rev. Lett.* **114**, 060402 (2015).
- [54] L. Rosales-Zárate, et al., *JOSA B* **32**, A82 (2015).
- [55] S. Kiesewetter et al., *SoftwareX*, March (2016).
- [56] K. E. Cahill and R. J. Glauber, *Phys. Rev.* **177**, 1882 (1969).
- [57] B. Schumacher, *Phys. Rev. A* **54**, 2614 (1996).
- [58] H. M. Wiseman, S. J. Jones, and A. C. Doherty, *Phys. Rev. Lett.* **98**, 140402 (2007); S. J. Jones, H. M. Wiseman, and A. C. Doherty, *Phys. Rev. A* **76**, 052116 (2007); E. G. Cavalcanti, S. J. Jones, H. M. Wiseman, M. D. Reid, *Phys. Rev. A* **80**, 032112 (2009).